Reply to "Comment on 'Characterizing ENSO Coupled Variability and Its Impact on North American Seasonal Precipitation and Temperature'"

MICHELLE L. L'HEUREUX

National Oceanic and Atmospheric Administration, NWS/NCEP/Climate Prediction Center, College Park, Maryland

MICHAEL K. TIPPETT

Department of Applied Physics and Applied Mathematics, Columbia University, New York, New York, and Center of Excellence for Climate Change Research, Department of Meteorology, King Abdulaziz University, Jeddah, Saudi Arabia

ANTHONY G. BARNSTON

International Research Institute for Climate and Society, Earth Institute, Columbia University, New York, New York

(Manuscript received 19 January 2016, in final form 25 August 2016)

We appreciate the opportunity to extend our analysis and examine the extent to which the central Pacific (CP) OLR index defined in L'Heureux et al. (2015, hereafter LTB15) is related to North American temperature and precipitation anomalies. We focus on the December–February (DJF) season for the period 1982–2014 and highlight the eight years classified in Harrison and Chiodi (2016, hereafter HC16), called HC16 OLR ENSO years. Here, we show the following: 1) The four El Niño and four La Niña years classified using two HC16 OLR indices correspond to the extreme positive and negative values of the CP OLR index. 2) The projection of observed North American DJF climate anomalies onto a CP OLR regression map of temperature or precipitation shows a linear relation with CP OLR. 3) Similar linear relationships are seen between CP OLR and North American climate anomalies even when the four El Niño or four La Niña years are excluded.

HC16 question the utility of linear analysis for studying the relation between ENSO and seasonal North American climate. Further, they recommend the use of their OLR El Niño and OLR La Niña indices instead of the CP OLR index of LTB15. While indices identical to those used in HC16 are not presented within (see HC16 and previous papers for details), Fig. 1 shows DJF values for 1982–2014 of two indices formed from seasonal averages of OLR over the regions used in HC16, an eastern Pacific (EP) and a western Pacific (WP) index. All OLR indices here are inverted (multiplied by −1). The four El Niño and four La Niña years discussed by HC16 are labeled on the EP and WP OLR figures, respectively. Large CP OLR amplitudes, positive and negative, are observed when there are large OLR values in the western and eastern Pacific as measured by the EP and WP indices. While not shown herein, CP OLR is also significantly correlated with the Niño-3.4 SST index ($r = 0.78$), which is often used in ENSO monitoring and prediction. Thus, a single index such as CP OLR captures a substantial portion of the relevant information and may have utility for applications.

For instance, the CP OLR index demonstrates a linear relationship with the regression pattern of seasonal climate impacts (Fig. 2). The top panels of Fig. 2 show the patterns obtained by regressing North American temperature and precipitation anomalies with CP OLR. The amplitude of the regression pattern in any particular DJF season is computed by projecting the anomalies of that season onto the regression map. The bottom panels of Fig. 2 show scatterplots of the projection coefficients and CP OLR. Large (small) projection

Corresponding author e-mail: Michelle L. L'Heureux, michelle.lheureux@noaa.gov

DOI: 10.1175/JCLI-D-16-0080.1

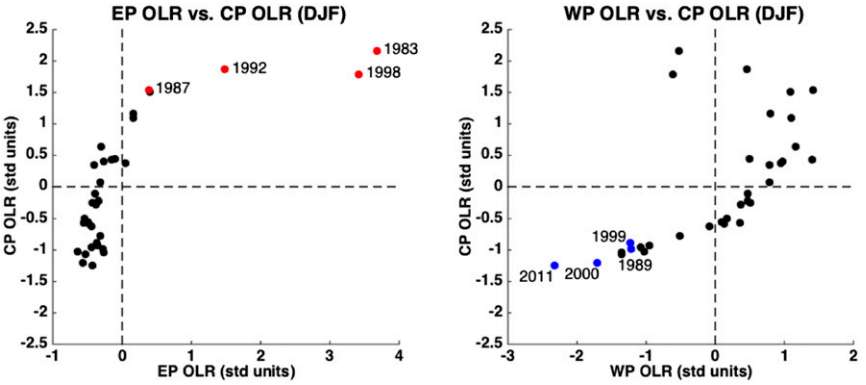

FIG. 1. Scatterplot of the DJF standardized CP OLR index on the ordinate and, on the abscissa, the standardized DJF (left) EP OLR index and (right) WP OLR index. The four El Niño years and four La Niña years identified by HC16 are noted by the red and blue dots, respectively. Anomalies are formed by removing monthly means of the full 1982–2014 period displayed here. The CP OLR region is 5°S–5°N, 170°E–140°W, the EP OLR region is 5°S–5°N, 160°–110°W, and the WP OLR region is 5°S–5°N, 150°E –180°. Monthly interpolated OLR data are from AVHRR (Liebmann and Smith 1996). All OLR indices are inverted (multiplied by −1).

coefficients correspond to larger (smaller) values of CP OLR and the scatterplots show linear relations, with the residuals about the least squares regression line consistent with a Gaussian distribution (not shown).

The same analysis using EP OLR finds regression patterns (Fig. 3, top panels) that are similar to the CP OLR regression patterns (Fig. 2, top panels). However, the scatterplots demonstrate strikingly nonlinear

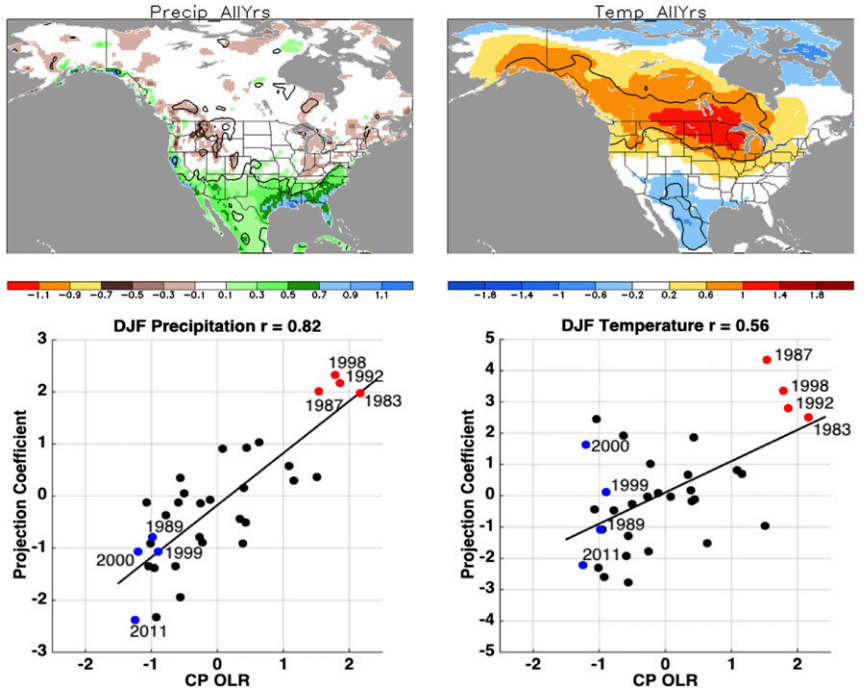

FIG. 2. DJF (top left) precipitation anomalies and (top right) temperature anomalies regressed onto the standardized CP OLR index. The solid contour shows where anomalies are 95% significant based on the Student's *t* test for the correlation coefficient. (bottom) The CP OLR index (abscissa) and the projection coefficients (ordinate) formed by projecting the anomalies from each DJF year onto the regression maps shown in (top). The correlation and least squares linear fit between the CP OLR index and the projection coefficient are also displayed. Data are from the CPC unified gauge-based precipitation dataset (Chen et al. 2008) and the combined Global Historical Climatology Network version 2 and Climate Anomaly Monitoring System (GHCN+CAMS) temperature dataset (Fan and van den Dool 2008). CP OLR is inverted (multiplied by −1).

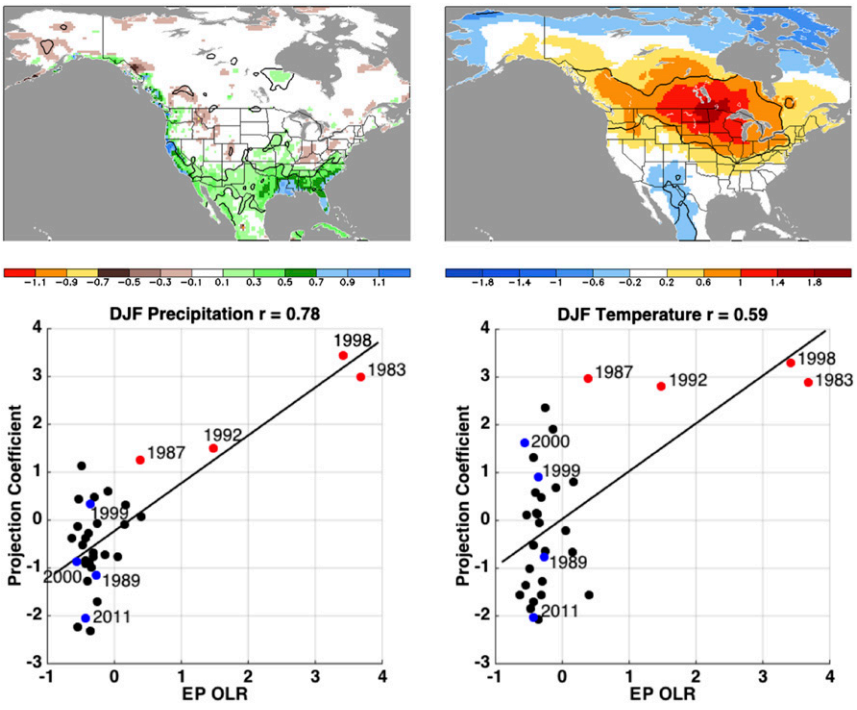

FIG. 3. As in Fig. 2, but using the standardized EP OLR index.

relationships between EP OLR and the projection of observed climate anomalies onto its regression maps (Fig. 3, bottom panels), in the sense that the four El Niño years identified by HC16 result in large projection coefficients, and the remaining years have widely varying projection coefficients for EP OLR values near zero. This behavior means that the EP OLR index provides little information about El Niño climate impacts in non-OLR El Niño years despite those years having climate anomalies that project onto the EP OLR regression maps. This characteristic of EP OLR index is not surprising because the index region was selected a posteriori to produce large values (relative to the rest of the time series) in only these years (see appendix 1 of Chiodi and Harrison 2013). However, the nonlinear behavior of EP OLR does not preclude other quantities, such as CP OLR, from having linear relationships with North American climate.

HC16 raise the question of whether ''non-OLR'' years (years outside of the identified four El Niño and four La Niña years) provide information about ENSO-related North American climate impacts. We explore the relative extent to which OLR ENSO years and non-OLR years provide information by repeating the CP OLR analysis (Fig. 2), but constructing the regression patterns first based on only either the four El Niño or the four La Niña years, and then based on the remaining years. This approach is not directly comparable to the bottom panel of Fig. 3 in HC16, which emphasizes the contemporaneous correlation, whereas our figures focus on the covariance between CP OLR and climate. Figure 4 shows North American precipitation results for the four El Niño years (left) and La Niña years (right), while Fig. 5 shows the same for temperature. The scatterplots show the projection coefficients obtained by projecting the observed anomaly (for each of the 33 years) onto the regression pattern formed from either the four El Niño or four La Niña years (patterns shown in the top panels and coefficients are shown by the filled circles and solid line in the bottom panels of Figs. 4 and 5) or the regression patterns formed from the remaining 29 years (patterns are not shown, but coefficients are indicated with open circles and a dashed line in the bottom panels of Figs. 4 and 5). The sample means are not removed, so the anomalies are with respect to the full 33-yr period.

In the case of precipitation (Fig. 4), the patterns are fairly similar regardless of whether El Niño, La Niña, or the remaining years are used, but the correlations based on the remaining years are slightly stronger, possibly due to the larger sample size. The slope of the regression line is more sensitive to the choice of years in the La Niña case. For temperature (Fig. 5), the El Niño case shows about equal correlation for both sets of years, although the slopes and spatial patterns differ

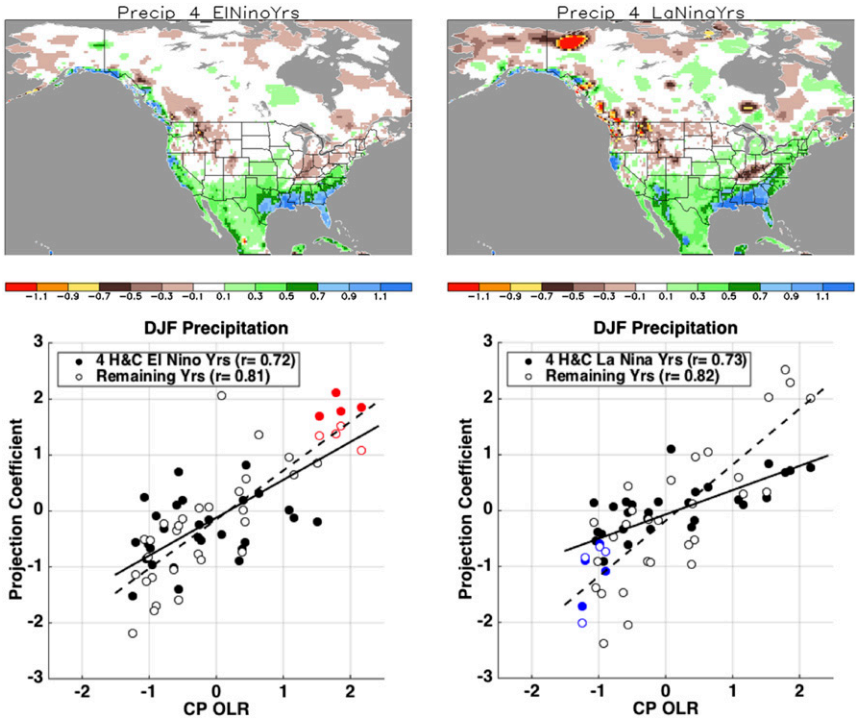

FIG. 4. As in Fig. 2, but showing DJF precipitation regressed onto CP OLR based on (top left) four El Niño years and (top right) four La Niña years. (bottom) Scatterplots showing the coefficients formed by projecting all 33 DJF cases onto the regression maps based on four El Niño years and four La Niña years (filled circles and solid line) and based on 29 remaining DJF cases in the 1982–2014 record (open circles and dashed line). The four HC16 El Niño years are shown at left in red while the four HC16 La Niña years are shown at right in blue.

somewhat. The disadvantage of using only four years to define the climate response is clearest in the case of the temperature regression patterns and scatterplots formed from the four La Niña years (Fig. 5; right panels) where the relatively weaker relation between U.S. temperature anomalies and La Niña deteriorates with small sample size. These results show the value of increased sample size when assessing ENSO-related climate impacts.

The nonlinear aspects of the connection between ENSO and North American temperature and precipitation anomalies are not easy to characterize from the limited historical record, where case-to-case variations include features of the climate system unrelated to ENSO (decadal changes, Arctic Oscillation (AO)/NAO states, anthropogenic forcing, etc.). The lack of clear ENSO-related impacts during a particular year could reflect other factors that mitigate or damp the expected ENSO signal (e.g., L'Heureux et al. 2010). Likewise, seemingly strong ENSO responses are difficult to disentangle from other relevant climate forcings. In other words, climate predictions are uncertain, even given the state of ENSO. We note that analysis here of simultaneous OLR and climate anomalies does not constitute prediction, although skillful predictions of North American climate based on Pacific SST have a long history (e.g., Barnston 1994).

Finally, recent work by Branstator (2014) provides a physical perspective by demonstrating that a heat source located in the eastern Pacific results in high-latitude wave trains that are less prominent than those forced from western and central Pacific heating (see Figs. 3 and 11 therein). Potentially, this difference in response may be because the wave train resulting from OLR forcing in the western and central tropical Pacific can tap into energy from the Asian Pacific jet (e.g., Simmons et al. 1983). So, while the central and eastern Pacific OLR anomalies can and certainly do coexist over the tropical Pacific, the evidence suggests that they may not be equally effective in driving impacts over remote locations.

Acknowledgments. We thank the editor and three reviewers for their suggestions. AGB acknowledges support from NOAA's Climate Program Office Modeling,

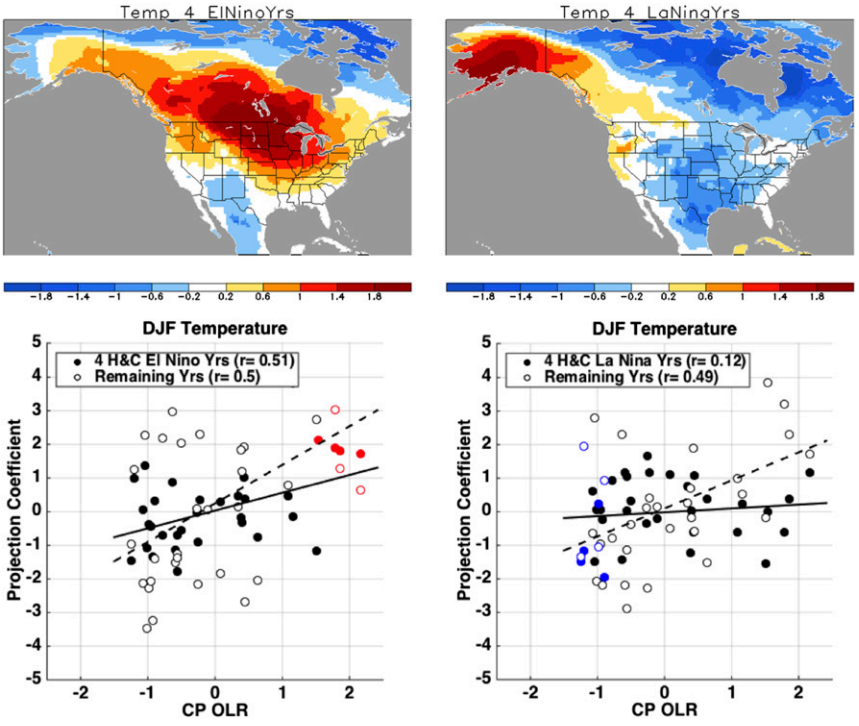

FIG. 5. As in Fig. 4, but showing DJF temperature.

Analysis, Predictions, and Projections Program Award NA12OAR4310082.

REFERENCES

Barnston, A. G., 1994: Linear statistical short-term climate predictive skill in the Northern Hemisphere. *J. Climate*, **7**, 1513–1564, doi:10.1175/1520-0442(1994)007<1513:LSSTCP>2.0.CO;2.

Branstator, G., 2014: Long-lived response of the midlatitude circulation and storm tracks to pulses of tropical heating. *J. Climate*, **27**, 8809–8826, doi:10.1175/JCLI-D-14-00312.1.

Chen, M., W. Shi, P. Xie, V. B. S. Silva, V. E. Kousky, R. W. Higgins, and J. E. Janowiak, 2008: Assessing objective techniques for gauge-based analyses of global daily precipitation. *J. Geophys. Res.*, **113**, D04110, doi:10.1029/2007JD009132.

Chiodi, A. M., and D. E. Harrison, 2013: El Niño impacts on seasonal U.S. atmospheric circulation, temperature, and precipitation anomalies: The OLR-event perspective. *J. Climate*, **26**, 822–837, doi:10.1175/JCLI-D-12-00097.1.

Fan, Y., and H. van den Dool, 2008: A global monthly land surface air temperature analysis for 1948–present. *J. Geophys. Res. Atmos.*, **113**, D01103, doi:10.1029/2007JD008470.

Harrison, D. E., and A. M. Chiodi, 2016: Comment on "Characterizing ENSO coupled variability and its impact on North American seasonal precipitation and temperature." *J. Climate*, **30**, 427–436, doi:10.1175/JCLI-D-15-0678.1.

L'Heureux, M., A. Butler, B. Jha, A. Kumar, and W. Wang, 2010: Unusual extremes in the negative phase of the Arctic Oscillation during 2009. *Geophys. Res. Lett.*, **37**, L10704, doi:10.1029/2010GL043338.

——, M. K. Tippett, and A. G. Barnston, 2015: Characterizing ENSO coupled variability and its impact on North American seasonal precipitation and temperature. *J. Climate*, **28**, 4231–4245, doi:10.1175/JCLI-D-14-00508.1.

Liebmann, B., and C. A. Smith, 1996: Description of a complete (interpolated) outgoing longwave radiation dataset. *Bull. Amer. Meteor. Soc.*, **77**, 1275–1277.

Simmons, A. J., J. M. Wallace, and G. W. Branstator, 1983: Barotropic wave propagation and instability, and atmospheric teleconnection patterns. *J. Atmos. Sci.*, **40**, 1363–1392, doi:10.1175/1520-0469(1983)040<1363:BWPAIA>2.0.CO;2.